12-31-2009

Electrical Impedance Imaging of Corrosion on a Partially Accessible 2-Dimensional Region

Court Hoang
Pomona College

Katherine Osenbach
University of Scranton

Advisors:
Kurt Bryan

MSTR 09-11

Electrical Impedance Imaging of Corrosion on a Partially Accessible 2-Dimensional Region

C. Hoang and K. Osenbach

Adviser: Kurt M. Bryan

Mathematical Sciences Technical Report Series
MSTR 09-11

December 31, 2009

Department of Mathematics
Rose-Hulman Institute of Technology
http://www.rose-hulman.edu/math

Fax (812)-877-8333 **Phone (812)-877-8193**

Electrical Impedance Imaging of Corrosion on a Partially Accessible 2-Dimensional Region

An Inverse Problem in Non-Destructive Testing

Court Hoang [1] **and Katherine Osenbach** [2]

Abstract

In this paper we examine the inverse problem of determining the amount of corrosion on an inaccessible surface of a two-dimensional region. Using numerical methods, we develop an algorithm for approximating corrosion profile using measurements of electrical potential along the accessible portion of the region. We also evaluate the effect of error on the problem, address the issue of ill-posedness, and develop a method of regularization to correct for this error. An examination of solution uniqueness is also presented.

[1] Pomona College
[2] The University of Scranton

1 Introduction

The ability to determine the size and location of defects on the interior of an object without destroying the object's integrity has many useful applications in industry today. Two of many methods for attacking this problem are impedance imaging and thermal imaging. In this paper, we will examine the use of steady state electrical impedance imaging to detect corrosion on the back surface of a region.

We will consider a region, Ω, that has a readily accessible top surface, but a completely inaccessible back surface. Our goal is to use measurements of electrical potential on the accessible surface to recover the profile of the corrosion on the back surface. That is, we will investigate how a corroded region, with a different electrical conductivity than that of the non-corroded region, impedes the flow of current from one portion of the surface to another. We will then use these impedance effects to reconstruct the corrosion profile knowing the conductivity of the corroded region, the input current profile, and the potential on the accessible surface.

2 The Forward Problem

Let Ω be a region in $\mathbb{R}^2$ defined in the following way: $\Omega = \{(x, y) : y \in [0, 1],\ \mathrm{x}\ \in (-\infty, \infty)\}$ (see Figure 1). Let Γ denote the upper boundary of Ω where $y = 1$. Let the curve $y = S(x)$ represent the upper boundary of a region $\Omega^- \subseteq \Omega$ such that $S(x)$ has compact support. Let $\Omega^+ = \Omega \backslash \Omega^-$. We assume Ω^+ has electrical conductivity equal to 1. We also assume Ω^-, which represents a region of corrosion along the back surface, has constant electrical conductivity γ not equal to 1.

A time-independent electrical flux, g, is applied to Γ. Assuming that the problem is steady-state, we then have functions of electrical potential, u^+ and u^-, in Ω^+ and Ω^-, respectively, satisfying the following partial differential equations (following from a standard model):

$$\Delta u^+ = 0, \text{ on } \Omega^+$$

$$\Delta u^- = 0, \text{ on } \Omega^-, \tag{2.1}$$

where Δu is the Laplacian of u. We also have the following boundary conditions:

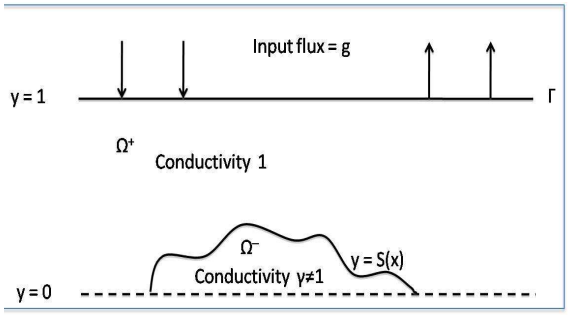

Figure 1: Diagram of the problem set-up.

$$\frac{\partial u^+}{\partial \vec{n}} = \nabla u^+ \cdot \vec{n} = g, \text{ on } \Gamma$$

$$\frac{\partial u^+}{\partial \vec{n}} = \nabla u^+ \cdot \vec{n} = 0, \text{ on } y = 0$$

$$\frac{\partial u^-}{\partial \vec{n}} = \nabla u^- \cdot \vec{n} = 0, \text{ on } y = 0$$

$$u^+ = u^-, \text{ on } y = S(x) \tag{2.2}$$

$$\frac{\partial u^+}{\partial \vec{n}} = \gamma \frac{\partial u^-}{\partial \vec{n}} \tag{2.3}$$

where $\vec{n}$ is an unit outward normal vector on Γ, $y = 0$, and $y = S(x)$. Equation (2.1) is known as Laplace's Equation. Functions that satisfy this equation are said to be *harmonic*.

Let us first consider the case where $\Omega^- = \emptyset$, that is there is no corrosion on the back surface of Ω. In this case, we will call the potential resulting from a non-corroded back surface u_0; note that u_0 will be defined on all of Ω. Now let us consider the case where $\Omega^- \neq \emptyset$, that is, some portion of the back surface of Ω is corroded.

This forward problem involves solving a system of partial differential equations given in equation (2.1) for the steady state electrical potential functions u^+ and u^- that satisfy the given boundary data detailed in equation (2.2). This forward problem is not the problem we analyzed. Instead, we will be investigating the following inverse problem: given information about u^+ on Γ, with known constant conductivity γ in Ω^-, and input flux g on Γ, we wish to approximate

the function $y = S(x)$.

3 Preliminary Information

Green's second identity will prove to be a useful tool for attacking the inverse problem. Let us recall Green's Second Identity: for any bounded region $D \subset \mathbb{R}^2$, with sufficiently smooth boundary ∂D, if $u, v \in C^2(D \cup \partial D)$, then

$$\iint_D (u\Delta v - v\Delta u)\, dA = \int_{\partial D} (u\frac{\partial v}{\partial \vec{n}} - v\frac{\partial u}{\partial \vec{n}})\, ds \tag{3.1}$$

where ds is the arc length element and $\vec{n}$ is the outward unit normal to ∂D. In our analysis, the function $v(x, y)$, which we refer to as the "test function", will be chosen to be harmonic. Green's second identity is a direct consequence of the Divergence Theorem, and will be used as the primary means of recovering the function $y = S(x)$.

4 Uniqueness

We will now discuss uniqueness for this inverse problem. In the linearized version of this problem (see Section 6), uniqueness of the corrosion profile $S(x)$ holds for a single measurement of data along the accessible surface Γ; however, in the non-linear version of the problem, it is very unlikely that a single measurement would assure uniqueness of S [1]. Though we do not have a complete uniqueness result, we show here that, in the non-linear version, if two profiles S_1 and S_2 generate the same data for u^+ along Γ, then S_1 and S_2 must have a non-zero point of intersection on their supported domains.

Suppose we have a region $\Omega \in \mathbb{R}^2$, bounded above by $\Gamma = \{(x, y) \colon y = 1\}$, and below by the line $y = 0$ (see Figure 2(a)). Given a function $u_1(x, y)$ defined on Ω and a curve $y = S_1(x) \not\equiv 0$ with compact support, suppose that the conductivity is 1 above $S_1(x)$ and $\gamma \neq 1$ below $S_1(x)$. Call u_1 above $S_1(x)$ u_1^+, and below $S_1(x)$, call it u_1^-. Suppose also that u_1 satisfies the following conditions:

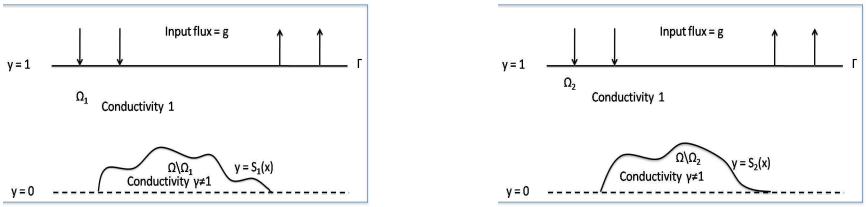

(a) Setup for u_1 with conductivity equal to 1 on Ω_1 and conductivity $\gamma \neq 1$ under $y = S_1(x)$.

(b) Setup for u_2 with conductivity 1 on Ω_2 and conductivity $\gamma \neq 1$ under $y = S_2(x)$.

Figure 2: Problem setup for u_1 and u_2.

$$\begin{gathered}
\Delta u_1 = 0 \text{ for } y > S_1(x) \text{ and } y < S_1(x), \\
\frac{\partial u_1}{\partial \vec{n}} = g \text{ on } \Gamma, \\
\frac{\partial u_1}{\partial \vec{n}} = 0 \text{ when } y = 0, \\
u_1^+ = u_1^- \text{ on } S_1(x) \text{ (i.e., } u_1 \text{ is continuous over } S_1(x)), \text{ and} \\
\frac{\partial u_1^+}{\partial \vec{n}} = \gamma \frac{\partial u_1^-}{\partial \vec{n}}.
\end{gathered} \tag{4.1}$$

Now, suppose we have another function $u_2(x, y)$ on Ω and another curve $S_2(x) \not\equiv 0$, also with compact support, such that u_2 satisfies the same conditions as u_1 with respect to S_2 (using the same boundary flux g and with the same value for γ under S_2; see Figure 2(b)). Let $\Omega_1, \Omega_2 \subseteq \Omega$ be the respective regions on which u_1 and u_2 have conductivity equal to 1 (see Figure 2). For the sake of simplicity, we assume that S_1 and S_2 are non-zero only on the intervals (a, b) and (c, d), respectively, and that they intersect at most once on $(a, b) \cup (c, d)$ (see Figures 2, 3). Let D_1 be the region enclosed by S_1 and S_2 when $S_1 > S_2$ (i.e., the region below S_1 and above S_2); let D_2 be the region enclosed by S_1 and S_2 when $S_1 < S_2$ (i.e., the region below S_2 and above S_1); let D_3 be the region below both S_1 and S_2 (see Figure 3). Note that any given D_k may be empty.

Claim. If $u_1 = u_2$ on any open portion of Γ, then there exists $x \in \mathbb{R}$ such that $0 \neq S_1(x) = S_2(x)$; that is, the non-zero portions of the graphs of S_1 and S_2

must intersect.

Proof. We begin with a statement of the following standard "unique continuation" lemma.

> **Lemma 1.** *Given a connected region Ω with C^2 boundary and functions u_1, u_2 with $\Delta u_{1,2} = 0$ in Ω, $\frac{\partial u_1}{\partial \vec{n}} = \frac{\partial u_2}{\partial \vec{n}}$ on an open subset Γ of the boundary of Ω, and $u_1 = u_2$ on Γ, then $u_1 = u_2$ everywhere in Ω.*

Now, suppose we have $u_1 = u_2$ on some open portion σ of Γ. Since $u_1 = u_2$ on σ, and because $\frac{\partial u_1}{\partial \vec{n}} = \frac{\partial u_2}{\partial \vec{n}} = g$ on all of Γ, it follows (by Lemma 1) that

$$u_1^+ = u_2^+ \text{ everywhere on } \Omega_1 \cap \Omega_2. \tag{4.2}$$

In this proof, we consider two cases: one in which S_1 and S_2 have disjoint supports (see Figure 3(b)); and one in which $S_1 \geq S_2$ everywhere (analogous to the case in which $S_2 \geq S_1$; see Figure 3(c)).

Case 1

In the first case, where $(a, b) \cap (c, d) = \emptyset$, we note first that $D_3 = \emptyset$ (see Figure 3(b)). Looking at D_1, we know that $\frac{\partial u_1}{\partial \vec{n}} = \frac{\partial u_2}{\partial \vec{n}} = 0$ along the back surface $y = 0$, and we also know by (4.1) and (4.2) that $u_1^- = u_1^+ = u_2^+$ on $S_1(x)$. Thus, we have the normal derivatives of u_1^- and u_2^+ equal to each other on part of the boundary of D_1, namely, on $y = S_1(x)$, and $u_1^- = u_2^+$ on another part of the boundary, namely, on $y = 0$. These two conditions are enough to ensure that, because both u_1 and u_2 satisfy Laplace's equation,

$$u_1 = u_2 \text{ everywhere in } D_1. \tag{4.3}$$

Similarly, we know that

$$u_1 = u_2 \text{ everywhere in } D_2. \tag{4.4}$$

Now, we know that D_1 or D_2 (or both) is non-empty. Without loss of generality, assume that $D_1 \neq \emptyset$. Then, by (4.3), we know that $u_1^- = u_2^+$ everywhere in D_1; by (4.2), $u_1^+ = u_2^+$ on $\Omega_1 \cap \Omega_2$. Thus $u_1^+ = u_1^- = u_2^+$ on Ω_2 (since u_2 is smooth over S_1), and so $\frac{\partial u_1^+}{\partial \vec{n}} = \frac{\partial u_1^-}{\partial \vec{n}}$ on Ω_2, contradicting our hypothesis (4.1) that $\frac{\partial u_1^+}{\partial \vec{n}} = \gamma \frac{\partial u_1^-}{\partial \vec{n}}$ (because $\gamma \neq 1$). We conclude that S_1 and S_2 cannot have

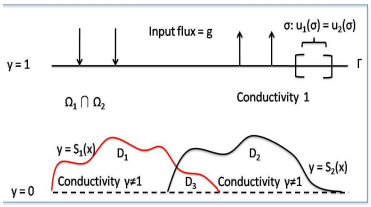

(a) With one non-zero intersection between S_1 and S_2.

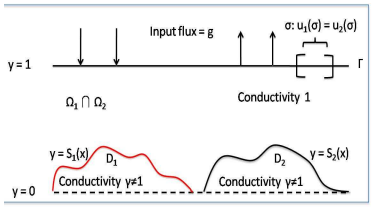

(b) Figure for Case 1 ($(a, b) \cap (c, d) = \emptyset$); note that here, $D_3 = \emptyset$.

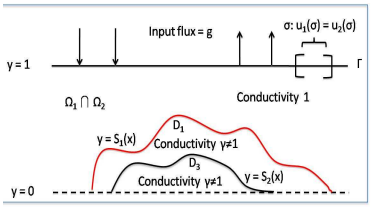

(c) Figure for Case 2 ($S_1 \geq S_2$ everywhere); note that here, $D_2 = \emptyset$.

Figure 3: Possible cases when S_1 and S_2 intersect non-trivially at most once.

disjoint support.

Case 2

In the second case, where $S_1 \geq S_2$ everywhere, we first note that $D_2 = \emptyset$, and that $D_3 \subset \Omega \backslash \Omega_1$ (see Figure 3(c)). Defining the functions γ_1 and γ_2 in accordance with our problem setup by

$$\gamma_k = \begin{cases} 1 & \text{in } \Omega_k, \\ \gamma & \text{in } \Omega \backslash \Omega_k, \end{cases}$$

we can restate the first condition (Laplace's equation) in our original boundary value problem (4.1) as

$$\nabla \cdot (\gamma_1 \nabla u_1) = 0 \text{ in } \Omega; \tag{4.5}$$

we can do the same for the boundary value problem with u_2 and S_2.

Suppose the solutions $u_{1,2}$ to these BVPs have Dirichlet boundary condition $u_1 = u_2 = f$ along $\partial\Omega = \Gamma \cup \{y = 0\}$, the boundary of Ω, for some $f \in C^1$ (we know that u_1 and u_2 must be defined by the same f by (4.2)). By Dirich-

let's Principle (see [2]), as solutions to these BVPs, u_1 and u_2 also minimize, respectively, the functionals

$$Q_1(\phi) = \int_\Omega \gamma_1 \left|\nabla\phi\right|^2 \, dA,$$

$$Q_2(\phi) = \int_\Omega \gamma_2 \left|\nabla\phi\right|^2 \, dA, \tag{4.6}$$

where ϕ is any function satisfying $\phi = f$ on $\partial\Omega$.

Consider the quantity

$$\int_{\partial\Omega} u_k \frac{\partial u_k}{\partial\vec{n}}, k = 1, 2.$$

This integral gives the power necessary to maintain the electrical current in Ω for u_1 or u_2. Now, along Γ, $u_1 = u_2$ (4.2), and $\frac{\partial u_1}{\partial\vec{n}} = \frac{\partial u_2}{\partial\vec{n}} = g$ (4.1). We also know by (4.1) that $\frac{\partial u_1}{\partial\vec{n}} = \frac{\partial u_2}{\partial\vec{n}} = 0$ along the back surface $y = 0$. Thus, for all of $\partial\Omega$, we have

$$\int_{\partial\Omega} u_1 \frac{\partial u_1}{\partial\vec{n}} \, ds = \int_{\partial\Omega} u_2 \frac{\partial u_2}{\partial\vec{n}} \, ds, \tag{4.7}$$

which implies

$$\int_\Omega \gamma_1 \left|\nabla u_1\right|^2 \, dA = \int_\Omega \gamma_2 \left|\nabla u_2\right|^2 \, dA$$

or, equivalently,

$$Q_1(u_1) = Q_2(u_2). \tag{4.8}$$

Suppose that $\gamma < 1$ (the case where $\gamma > 1$ yields an analogous contradiction). Then, because $D_3 \subset D_1$ (i.e., the area under S_1 is greater than that of S_2), $\gamma_1 \leq \gamma_2$ everywhere on Ω, and equality holds everywhere except on D_1. Then, for any ϕ with $\phi = f$ on $\partial\Omega$, it must be that

$$\int_\Omega \gamma_1 \left|\nabla\phi\right|^2 \, dA \leq \int_\Omega \gamma_2 \left|\nabla\phi\right|^2 \, dA. \tag{4.9}$$

In fact, equality only holds in (4.9) if ϕ is constant on D_1: since equality between γ_1 and γ_2 holds except on D_1, we would need to have

$$\int_{D_1} \gamma_1 \left|\nabla\phi\right|^2 \, dA = \int_{D_1} \gamma_2 \left|\nabla\phi\right|^2 \, dA,$$

or

$$\int_{D_1} \gamma \left|\nabla\phi\right|^2 \, dA = \int_{D_1} 1 \cdot \left|\nabla\phi\right|^2 \, dA$$

(since $\gamma_1 = \gamma, \gamma_2 = 1$ on D_1), so

$$\int_{D_1} (\gamma - 1) \left|\nabla\phi\right|^2 \, dA = 0.$$

Since $\gamma \neq 1$, then $|\nabla\phi| = 0$, so ϕ must be constant on D_1.

Because u_2 satisfies Laplace's equation, we cannot have u_2 constant on D_1 or it would be constant everywhere on Ω. Thus, by (4.9), we may say that

$$Q_2(u_2) = \int_\Omega \gamma_2 \left|\nabla u_2\right|^2 \, dA > \int_\Omega \gamma_1 \left|\nabla u_2\right|^2 \, dA. \tag{4.10}$$

Because u_1 minimizes $Q_1(u_1)$ as defined in (4.6), we know that

$$Q_1(u_1) = \int_\Omega \gamma_1 \left|\nabla u_1\right|^2 \, dA \leq \int_\Omega \gamma_1 \left|\nabla u_2\right|^2 \, dA. \tag{4.11}$$

Combining (4.10) and (4.11) yields

$$Q_2(u_2) > \int_\Omega \gamma_1 \left|\nabla u_2\right|^2 \, dA \geq Q_1(u_1), \tag{4.12}$$

contradicting (4.8).

Thus, in either case, we reach a contradiction, and so there must be a non-zero point of intersection between S_1 and S_2; more precisely, S_1 and S_2 cannot have disjoint supports, and neither can lie entirely above the other. □

5 Recovering $S(x)$

Our goal is to reconstruct the function $y = S(x)$ which determines the corroded surface Ω^-. To this end, we will use Green's second identity (3.1), with a test function $v(x, y)$ satisfying the following conditions:

$$\begin{aligned} \Delta v(x,y) &= 0, \\ \frac{\partial v}{\partial \vec{n}} &= 0 \text{ when } y = 0. \end{aligned} \tag{5.1}$$

Both $u(x, y)$ and $v(x, y)$ are harmonic functions. The left hand side of equation (3.1) thus becomes identically 0; applying this on the region Ω_1 and substituting the fact that $\frac{\partial u^+}{\partial \vec{n}} = g$ on Γ yields:

$$0 = \int_\Gamma u^+ \frac{\partial v}{\partial \vec{n}} - vg \, ds - \int_S u^+ \frac{\partial v}{\partial \vec{n}} - v \frac{\partial u^+}{\partial \vec{n}} \, ds \tag{5.2}$$

On the region Ω^-, knowing that $\frac{\partial u^-}{\partial \vec{n}} = 0$ on $y = 0$ and $\frac{\partial u^-}{\partial \vec{n}} = \frac{1}{\gamma}\frac{\partial u^+}{\partial \vec{n}}$ on $y = S(x)$, we will again apply Green's second identity to obtain:

$$0 = \int_{y=S(x)} u^- \frac{\partial v}{\partial \vec{n}} - v\frac{1}{\gamma}\frac{\partial u^+}{\partial \vec{n}}\, ds - \int_{y=0} u^- \frac{\partial v}{\partial \vec{n}} - v\frac{1}{\gamma}\frac{\partial u^+}{\partial \vec{n}}\, ds \tag{5.3}$$

The goal is to obtain an equation in which we have known, or calculable, quantities equal to the unknown S function. To this end, add equations (5.2) and (5.3) to obtain the following:

$$\int_\Gamma u^+ \frac{\partial v}{\partial \vec{n}} - vg\, ds - \int_{y=0} u_2 \frac{\partial v}{\partial \vec{n}}\, ds = \int_{y=S(x)} (u^+ - u^-)\frac{\partial v}{\partial \vec{n}} + v(1 - \frac{1}{\gamma})\frac{\partial u^+}{\partial \vec{n}}\, ds.$$

Because we chose the test function v such that $\frac{\partial v}{\partial \vec{n}} = 0$ on $\{y = 0\}$, this gives the following simplified equation:

$$\int_\Gamma u^+ \frac{\partial v}{\partial \vec{n}} - vg\, ds - \int_{y=0} u^- \frac{\partial v}{\partial \vec{n}}\, ds = \int_{y=S(x)} v(1 - \frac{1}{\gamma})\frac{\partial u^+}{\partial \vec{n}}\, ds. \tag{5.4}$$

An alternate form of equation (5.4) can be obtained by multiplying equation (5.3) by γ and then adding it to equation (5.2). This results in the following:

$$\int_\Gamma u^+ \frac{\partial v}{\partial \vec{n}} - vg\, ds - \gamma \int_{y=0} u^- \frac{\partial v}{\partial \vec{n}}\, ds = \int_{y=S(x)} \gamma u^- \frac{\partial v}{\partial \vec{n}} - v\frac{\partial u^+}{\partial \vec{n}} - u^+ \frac{\partial v}{\partial \vec{n}} + v\frac{\partial u^+}{\partial \vec{n}}\, ds.$$

But $u^+ = u^-$ on $y = S(x)$, and we chose v such that $\frac{\partial v}{\partial \vec{n}} = 0$ on S; therefore, we have:

$$\underbrace{\int_\Gamma \left(u^+ \frac{\partial v}{\partial \vec{n}} - vg \right) ds}_{RG(v)} = \int_{y=S(x)} (\gamma - 1) u^+ \frac{\partial v}{\partial \vec{n}}\, ds \tag{5.5}$$

The left side of equation (5.5) is often referred to as the reciprocity gap integral. We will hereby refer to it as $RG(v)$ throughout the remainder of this paper. $RG(v)$ is a computable quantity for any chosen harmonic test function v from the known boundary data u^+ and input flux g. We thus have

$$RG(v) = \int_{y=S(x)} (\gamma - 1) u^+ \frac{\partial v}{\partial \vec{n}}\, ds \tag{5.6}$$

Let us write equation (5.6) out a bit more explicitly. A unit normal vector to the curve $y = S(x)$, pointing upward, is of the following form:

$$\vec{n} = \frac{< -S'(x), 1 >}{\sqrt{1 + (S'(x))^2}}$$

the ds arc length factor is:

$$ds = \sqrt{1 + (S'(x))^2}\, dx \tag{5.7}$$

Multiplying $\frac{\partial v}{\partial \vec{n}} = \nabla v \cdot \vec{n}$ by the differential ds yields:

$$\frac{\partial v}{\partial \vec{n}}\, ds = \frac{-S'(x)\frac{\partial v}{\partial x} + \frac{\partial v}{\partial y}}{\sqrt{1 + (S'(x))^2}} \cdot \sqrt{1 + (S'(x))^2}\, dx = -S'(x)\frac{\partial v}{\partial x} + \frac{\partial v}{\partial y}\, dx \tag{5.8}$$

Substituting this into the right side of equation (5.6) we obtain:

$$RG(v) = (\gamma - 1) \int_{-\infty}^{\infty} -u^+(x, S(x))S'(x)\frac{\partial v}{\partial x}(x, S(x)) + u^+(x, S(x))\frac{\partial v}{\partial y}(x, S(x))\, dx \tag{5.9}$$

We now have reached the desired goal of known quantities on one side of the equation, and the unknown function S on the other. Given information about the potential on Γ, the electrical conductivity γ in Ω^-, the general procedure is to use equation (5.9), with an appropriate variety of test functions v, to collect information about the function $y = S(x)$ which defines the corroded region Ω^-. One difficulty is that the function S appears inside u^+, a quantity not know to us. The problem can be overcome by linearizing, as we show below.

6 Linearization

How can we use (5.9) to obtain an accurate approximation of the S function? To answer this question will implement the following two procedures - linearization and regularization.

We will begin with the process of linearization (regularization will be discussed in Section 12). Recall right side of equation (5.9). We will make the assumption that the corrosion profile is close to zero, that is, assume that $S = \varepsilon S_0$ for some "base profile" S_0. Let us first examine the case where $\varepsilon = 0$. If $\varepsilon = 0$ then $S = 0$, and we have:

$$(\gamma - 1) \int_{-\infty}^{\infty} u(x, 0) v_y(x, 0)\, dx = 0. \tag{6.1}$$

The case where $\varepsilon > 0$, requires the following intuitive approximation: $u^+(x, \varepsilon S_0(x)) \approx u_0(x, \varepsilon S_0(x))$ for ε small. This approximation can be quantitatively justified,

but this is beyond the scope of our work. Under this approximation, however, the right side of equation (5.9) becomes:

$$(\gamma - 1) \int_{-\infty}^{\infty} u_0(x, \varepsilon S_0(x)) \Big[- \varepsilon S_0'(x) v_x(x, \varepsilon S_0'(x)) + v_y(x, \varepsilon S_0'(x)) \Big] \, dx. \quad (6.2)$$

We will now perform a Taylor series expansion on the right side of the expression in (6.2) about $\varepsilon = 0$ in order to linearize the problem for further analysis.

The Taylor series expression for $u_0(x, \varepsilon S_0(x))$ about $\varepsilon = 0$ is:

$$\begin{aligned} u_0(x, \varepsilon S_0(x) &= u_0(x,0) + \varepsilon \frac{\partial u_0}{\partial y} \mid_{(x,0)} S_0(x) + \frac{1}{2} \varepsilon^2 \frac{\partial^2 u_0}{\partial^2 y} \mid_{(x,0)} + O(\varepsilon^3) \\ &= u_0(x, \varepsilon S_0(x)) + \frac{1}{2} \varepsilon^2 \frac{\partial^2 u_0}{\partial^2 y} \mid_{(x,0)} + O(\varepsilon^3), \end{aligned}$$

because of the insulating boundary condition $\frac{\partial u_0}{\partial y}\big|_{(x,0)} = 0$.

The Taylor series expression for $-\varepsilon S_0'(x) v_x(x, \varepsilon S_0(x))$ is

$$-\varepsilon S_0'(x) v_x(x, \varepsilon S_0(x)) = -\varepsilon S_0'(x) v_x(x,0) - \varepsilon^2 S_0'(x) v_{xy}(x,0) S_0(x) - O(\varepsilon^3).$$

The Taylor series expression for $v_y(x, \varepsilon S_o(x)$ is

$$v_y(x, \varepsilon S_0(x) = v_y(x,0) + \varepsilon S_0(x) v_{yy}(x,0) + \frac{\varepsilon^2}{2} (S_0(x))^2 v_{yyy}(x,0) + O(\varepsilon^3).$$

We can now substitute these Taylor expressions into equation (6.2) to obtain:

$$(\gamma - 1) \int_{-\infty}^{\infty} \Big[u_0(x,0) + \varepsilon \frac{\partial u_0}{\partial y} \mid_{(x,0)} S_0(x) + \frac{1}{2} \varepsilon^2 \frac{\partial^2 u_0}{\partial^2 y} \mid_{(x,0)} + O(\varepsilon^3) \Big] \Big[-\varepsilon S_0'(x) v_x(x,0)$$

$$- \varepsilon^2 S_0'(x) v_{xy}(x,0) S_0(x) + v_y(x,0) + \varepsilon S_0(x) v_{yy}(x,0) + \frac{\varepsilon^2}{2} (S_0(x))^2 v_{yyy}(x,0) + O(\varepsilon^3) \Big] \, dx.$$

Multiplying through, and grouping terms according to order of ε, we have:

$$(\gamma - 1) \int_{-\infty}^{\infty} \varepsilon \Big(u_0(x,0) \Big[S_0(x) v_{yy}(x,0) - S_0'(x) v_x(x,0) \Big] + S_0(x) v_y(x,0) \frac{\partial u_0}{\partial y} \mid_{(x,0)} \Big) + O(\varepsilon^2) \, dx.$$

Note that the zero-order term $(\gamma - 1) \int_{-\infty}^{\infty} u_0(x,0) \cdot v_y(x,0)$ is zero by our choice of v and equation (6.1).

Terms of order ε^2 and higher can be ignored for ε small without greatly affecting the approximation. Under this assumption, the right side of (5.9) becomes

$$(\gamma-1)\varepsilon\int_{-\infty}^{\infty}u_0(x,0)\Big[S_0(x)v_{yy}(x,0)-S_0'(x)v_x(x,0)\Big]+S_0(x)v_y(x,0)\frac{\partial u_0}{\partial y}\mid_{(x,0)}\,dx.$$

Now recall our choice of $v(x,y)$ such that $v_y(x,0)=0$. Equation (5.9) becomes

$$RG(v)\approx(\gamma-1)\epsilon\int_{-\infty}^{\infty}u_0(x,0)\Big[S_0(x)v_{yy}(x,0)-S_0'(x)v_x(x,0)\Big]\,dx. \tag{6.3}$$

Since $v(x,y)$ satisfies Laplace's equation, we know that $v_{yy}(x,y)=-v_{xx}(x,y)$ on Ω^+ and Ω^-, and so we can substitute in the right side of the approximation (6.3) to obtain:

$$(\gamma-1)\epsilon\int_{-\infty}^{\infty}-u_0(x,0)[S_0(x)v_{xx}(x,0)+S_0'(x)v_x(x,0)]\,dx.$$

Letting $h(x)=v(x,0)$, we can use the product rule in one dimension to obtain:

$$-(\gamma-1)\epsilon\int_{-\infty}^{\infty}u_0(x,0)\Big[S_0(x)h''(x)+S_0'(x)h'(x)\Big]\,dx$$

$$=-(\gamma-1)\epsilon\int_{-\infty}^{\infty}u_0(x,0)\frac{d}{dx}\Big[S_0(x)h'(x)\Big]\,dx.$$

Using differentiation by parts, $\int udv=uv-\int vdu$, with $u=u_0(x,0)$ and $dv=\frac{d}{dx}[S_0(x)h'(x)]$, we get:

$$-(\gamma-1)\epsilon\Big[u_0(x,0)S_0(x)h'(x)\Big|_{-\infty}^{\infty}+\int_{-\infty}^{\infty}\frac{\partial u_0}{\partial x}\mid_{(x,0)}\,S_0(x)h'(x)\,dx\Big].$$

Substituting $v(x,0)=h(x)$ back in yields:

$$-(\gamma-1)\epsilon\Big[u_0(x,0)S_0(x)v_x(x,0)\Big|_{-\infty}^{\infty}+\int_{-\infty}^{\infty}\frac{\partial u_0}{\partial x}\mid_{(x,0)}\,S_0(x)v_x(x,0)\,dx\Big]. \tag{6.4}$$

Assuming that our function $S_0(x)$ has compact support, the first term of (6.4) is zero when evaluated from $-\infty$ to ∞. We are left with:

$$-(\gamma-1)\epsilon\int_{-\infty}^{\infty}\frac{\partial u_0}{\partial x}(x,0)S_0(x)v_x(x,0)\,dx. \tag{6.5}$$

Finally, we can substitute (6.5) back into equation (5.9) to obtain:

$$\begin{aligned} RG(v) &\approx -(\gamma-1)\epsilon \int_{-\infty}^{\infty} \frac{\partial u_0}{\partial x}(x,0) S_0(x) v_x(x,0)\, dx. \\ &= (1-\gamma) \int_{-\infty}^{\infty} \frac{\partial u_0}{\partial x}(x,0) \frac{\partial v_k}{\partial x}(x,0) S(x)\, dx \end{aligned} \tag{6.6}$$

Equation (6.6) is the fully linearized version of our original reciprocity gap equation (5.9). Once again, note that $RG(v)$ is calculable: we choose $v(x,y)$, and we can compute $u_0(x,y)$ on Γ. Thus the linearized equation allows us to numerically solve for the function S that defines the corrosion.

We should note that it can be shown, using an integration-by-parts argument similar to the reciprocity gap argument above, that we can also compute $RG(v)$ as

$$RG(v) = \int_{\Gamma} \left(\tilde{u} \frac{\partial v}{\partial \mathbf{n}} - vg \right) ds \tag{6.7}$$

where $\tilde{u}$ is the function defined on $\Omega = (-\infty, \infty) \times (0,1)$ that satisfies

$$\triangle \tilde{u} = 0 \text{ in } \Omega \tag{6.8}$$

$$\frac{\partial \tilde{u}}{\partial \mathbf{n}} = 0 \text{ on } y = 1 \tag{6.9}$$

$$\frac{\partial \tilde{u}}{\partial \mathbf{n}} = -\frac{\partial}{\partial x} \left(S_0(x) \frac{\partial u_0}{\partial x}(x,0) \right) \text{ on } y = 0. \tag{6.10}$$

The problem (6.8)-(6.10) is the linearized (with respect to $S = 0$) version of the original problem stated in Section 2.

7 Approximating the Corrosion Profile

In the previous section, we derived a linearized version (6.6) of our original reciprocity gap integral equation (5.9), when the appropriate test function v is chosen. Using this linearized equation, we can use numerical methods to produce a function approximating the curve $y = S(x)$, and thus we can obtain an approximate image of the corrosion profile on the inaccessible surface. To this effect, we group the known quantities on the right side of equation, which becomes

$$RG(v) = -(\gamma - 1) \int_{-\infty}^{\infty} w(x) S(x)\, dx, \tag{7.1}$$

where $w(x) = \frac{\partial u_0}{\partial x}(x,0)v_x(x,0)$. As we choose test functions v_j, we refer to their respective w functions as w_j (i.e., $w_j(x) = \frac{\partial u_0}{\partial x}(x,0)\frac{\partial v_j}{\partial x}(x,0)$).

We choose a number, n, of test functions $v_j, j = 1, ..., n$, and we obtain a system of n linear equations:

$$\begin{aligned} RG(v_1) &= (1-\gamma)\int_{-\infty}^{\infty} w_1(x)S(x)\,dx, \\ RG(v_2) &= (1-\gamma)\int_{-\infty}^{\infty} w_2(x)S(x)\,dx, \\ &... \\ RG(v_n) &= (1-\gamma)\int_{-\infty}^{\infty} w_n(x)S(x)\,dx. \end{aligned} \tag{7.2}$$

Now, we know $RG(v_j)$ and $w_j(x)$ for $j = 1, ..., n$. We wish to find a function $S(x)$ that satisfies these equations and minimizes $\|S(x)\|_2$, the L^2-norm of $S(x)$. We use the L^2-norm because it produces a more elegant solution, and because it gives a lower-bound for severity of the corrosion. It is shown in the following section that such an S is unique and of the form

$$S(x) = \sum_{j=1}^{n} c_j w_j(x), \tag{7.3}$$

where the numerical coefficients c_j are as yet unknown. Substituting (7.3) into (7.2), we obtain a system of n equations with n unknowns c_j. Solving this system of equations yields the c_j, giving us an approximation for $S(x)$ as a linear combination of the functions $w_j(x)$.

7.1 Proof of How to Find the Minimum Norm Linear Approximation of The Function $y = S(x)$

Let S be a function defined on an interval I. Suppose:

$$\int_I w_k(x)S(x)\,dx = a_k \tag{7.4}$$

for $k = 1$ to n, where the w_k and a_k functions are known. Also recall that the $L^2(I)$ norm is given by

$$\|S(x)\|_2 = \sqrt{\int_I S^2(x)\,dx},$$

and that the inner product of two functions $f, g \in L^2(I)$ is

$$< f, g >= \int_I f(x)g(x)\,dx,$$

assuming, as we are, that the functions are real-valued.

Claim: If the $w_k \in L^2(I)$, then the function S which is consistent with the data in equations (7.1) and has the smallest L^2-norm is of the form:

$$S(x) = \sum_{k=1}^{n} \lambda_k w_k(x) \tag{7.5}$$

for some constants λ_k.

Proof. Assume $S(x)$ is defined on an interval I and we are given (7.4). The set of functions $w_1, w_2, ..., w_n$ can be extended to a basis for $L^2(I)$ by adding $w_{n+1}, w_{n+2}, ...$ These additional basis functions can be chosen such that they are orthogonal to the first n functions. Thus any function $S \in L^2(I)$ can be expressed as:

$$S(x) = \sum_{j=1}^{n} \lambda_j w_j(x) + r(x) \tag{7.6}$$

where $r(x) = \sum_{j=n+1}^{\infty} \lambda_j w_j(x)$. Note that $< r, w_j >= 0$ for $j \leq n$.

Then (7.4) becomes:

$$\sum_{j=1}^{n} < w_k, w_j > \lambda_j = a_k$$

which is a system of n equations with n unknowns λ_j, $j = 1$ to $j = n$. This system uniquely determines the λ_j, at least if the equations are not singular. So the first n of the λ_j in (7.6) are forced by the constraints. We want to choose the remaining λ_j to minimize $\|S\|_2$. But we can see that:

$$\|S\|_2^2 = \left\| \sum_{j=1}^{n} \lambda_j w_j \right\|^2 + \|r\|^2$$

Since the $\lambda_1, ..., \lambda_n$ are fixed, $\|S\|_2^2$ can only be changed by changing $\|r\|$. To minimize $\|S\|_2$, we of course take $r = 0$. Thus the function S which is consistent with the data and has the smallest L^2-norm is of the form:

$$S(x) = \sum_{k=1}^{n} \lambda_k w_k(x)$$

. □

8 Program Outline

We designed a Maple program to approximate the function $y = S(x)$ using the calculations shown above. For any given set of data taken on the accessible surface Γ of Ω, the program generates a function $S(x)$ that approximates the contour of the corrosion present on the inaccessible back surface of Ω. The data is generated assuming a particular input flux g thus also determining the function $u_0(x, y)$.

We must first generate the system of equations to be solved by calculating the $RG(v)$ values and the $w(x)$ functions. To this end, we must choose test functions $v(x, y)$ that satisfy the conditions expressed in (5.1), and we must also select the number of these functions to be used. Once the test functions are chosen, we will numerically compute the reciprocity gap integrals using the discrete data points generated on Γ. The integrals will then be evaluated, using the midpoint rule, as sums in the following way:

$$RG(v_k) = \frac{2A}{M(1-\gamma)} \sum_{j=1}^{M} -\frac{\partial v_k}{\partial \vec{n}}(X_j, 1)(u_j - u_o(X_j, 1)), \tag{8.1}$$

where X_j are the x-coordinates of the measured data points u_j, and M is the total number of data points generated on the interval $[-A, A]$.

The w_j functions were then calculated according to how they were defined in (7.1). The coefficient matrix, B, was constructed in the following way:

$$B = \begin{bmatrix} \int_{-A}^{A} w_1 w_1 dx & \int_{-A}^{A} w_2 w_1 dx & \cdots & \int_{-A}^{A} w_n w_1 dx \\ \int_{-A}^{A} w_1 w_2 dx & \int_{-A}^{A} w_2 w_2 dx & \cdots & \int_{-A}^{A} w_n w_2 dx \\ \vdots & & & \\ \int_{-A}^{A} w_n w_1 dx & \int_{-A}^{A} w_2 w_n dx & \cdots & \int_{-A}^{A} w_n w_n dx \end{bmatrix} \tag{8.2}$$

The column vector, $\vec{a}$, has entries $a_k = RG(v_k)$. The system

$$B\vec{c} = \vec{a} \tag{8.3}$$

was solved to determine the entries c_j of the vector $\vec{c}$.

We then generated an approximation of the $S(x)$ function via linear combi-

nation in the following way:

$$S(x) \approx \sum_{k=1}^{n} w_k c_k \tag{8.4}$$

where n is the number of test functions used. We then plotted this approximation to get a graphical representation of the corroded back surface of the region Ω.

9 A Numerical Example

We will now present an example with simulated data based on the linearized version of the forward problem. More precisely, we chose a function S, used the boundary value problem (6.8)-(6.10) and equation (6.7) to generate the $RG(v_k)$ values, and then used the procedure above to recover and estimate of S from this simulated data. We generated data along Γ of the electrical potential $u(x, y)$ at 200 evenly spaced points on the domain [-10,10], with noise added at each point of magnitude 0.01. This allows us to focus on the stability of the inversion procedure without dealing the with error introduced by the linearization. (We examine fully nonlinear versions below.) The data was generated using the input flux

$$g(x) = \frac{\partial u_0}{\partial \vec{n}}(x, 1),$$

where u_0, the function of electrical potential in the case with no corrosion, was given by:

$$u_0(x, y) = \text{Im}\left(\frac{1}{(x + iy - 1.2i)^2} + \frac{1}{(x - iy - 1.2i)^2}\right)$$

The function u_0 is harmonic, with normal derivative equal to 0 along the back surface (where $y = 0$), and real-valued. For a graph of $u(\Gamma) - u_0(\Gamma)$, using this u_0 function and the measured data points u along Γ, see Figure 4.

We assume the conductivity in the corroded region to be $\gamma = 0.1$. We vary the number, n, of test functions v_j, each with the general form

$$v_j(x, y) = \text{Im}\left(\frac{1}{\frac{10j+n-11}{n-1} - 6 + x + iy - 2i} + \frac{1}{\frac{10j+n-11}{n-1} - 6 + x - iy - 2i}\right).$$

These functions are chosen to be harmonic, with normal derivative equal to 0 along the back surface $\{y = 0\}$, real-valued, and so that the collection of test

functions is evenly and symmetrically spaced across the y-axis (symmetry is also ensured by our choice of $n = 10 * m + 1$ for $m \in \mathbb{N}$). The graphs of $v_j(x)$ for $j = 1, ..., n$, $x \in [-10, 10]$ when $n = 11$ are plotted against each other in Figure 5.

A graph of the approximated corrosion profile, using the same measurements of u and the same type and number of test functions v_j as in Figures 4 and 5, can be seen in Figure 6. This approximation of S is unreasonable due to the ill-posedness of this problem which is examined in the next section.

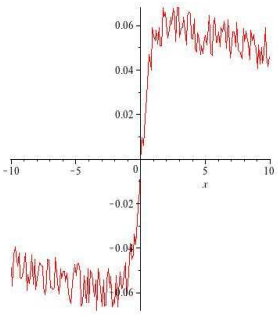

Figure 4: A graph of the difference $u(\Gamma) - u_0(\Gamma)$ along the top surface Γ with the generated measurements of u used in Section 9.

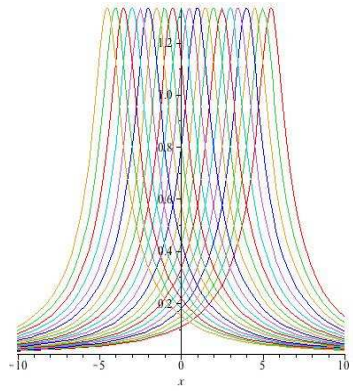

Figure 5: Graphs of the test functions $v_j(x)$ with $j = 1, ..., 11$, as defined in Section 9, plotted against each other (the index j is increasing from left to right).

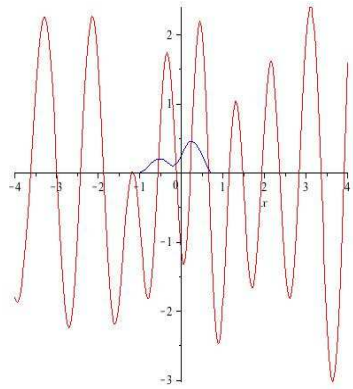

Figure 6: A graph of the approximated corrosion profile with data and test functions from Section 9.

10 Ill-Posedness

The ill-posedness of this inverse problem can be most clearly seen in analysis of the Fourier Series expansion. Recall the definition of the Fourier Series: if $f(x)$ is a piecewise-smooth, 2π-periodic continuous function defined on the interval $[-\pi, \pi]$, then it can be represented as a Fourier Series on this interval in the following way:

$$f(x) = \frac{a_0(f)}{2} + \sum_{n=1}^{\infty} a_n(f)\cos nx + b_n(f)\sin nx$$

where the Fourier coefficients a_n and b_n are given by:

$$a_n(f) = \frac{1}{\pi}\int_{-\pi}^{\pi} f(x)\cos nx\,dx, \text{ for n} \geq 0,$$

$$b_n(f) = \frac{1}{\pi}\int_{-\pi}^{\pi} f(x)\sin nx\,dx, \text{ for n} \geq 1.$$

Due to the applied nature of this problem, we can expect some error to be involved in our data. We will assume no error in the input flux g on Γ because we choose g specifically, but there will be some error of magnitude ε in the measurement of u on Γ. That is, instead of measuring u on Γ we are in fact measuring $\tilde{u} = u + \varepsilon(x)$. This error is either due to noise in the data itself, or noise generated by rounding errors in computing. The error in u results in an error in the computed Fourier coefficients of S; instead of computing the true coefficient a_k, we will actually compute $\tilde{a_k} = a_k + \varepsilon_k$, where ε_k is some error. In most inverse problems, including this one, the computation of $\tilde{a_k}$ becomes more unstable as the value of k increases. In fact, we find that, in the worse case:

$$\varepsilon_k \approx 2kM\varepsilon_\infty \tag{10.1}$$

where k is an integer, M is the number of terms chosen, and ε_∞ is the supremum of ε_k over the interval $[-M, M]$. This will be shown in the next section.

From (10.1), it is evident that $|\varepsilon_k|$ increases linearly with the number of Fourier coefficients chosen. Therefore, for large enough M values, our $\tilde{a_k}$ estimates are comprised almost entirely of noise and provide little information about the true a_k values. This means that, after a certain M value, trying to reconstruct S using $\tilde{a_k}$ will prove futile. This is the ill-posedness of the inverse problem. Increasing the number of test functions used increases the precision

information gleaned about S. However, this information is corrupted by the noise present in the data.

11 Error Analysis

Let us examine the effect of noise on the approximation in greater detail. Recall equation (6.6). We can calculate all of the $RG(v_k)$, so we will now refer to them as a_k. We will also assume support of S on the interval $[0, \pi]$. That is, S is non-zero in this interval. For this analysis it will be easier to consider test functions $v_k(x, y)$ of the following form,

$$v_k(x, y) = \frac{\cos(kx)\cosh(ky)}{\cosh(k)} \tag{11.1}$$

where k is an integer, and division by $\cosh(k)$ was performed so that $v(x, 1) = \cos(kx)$.

Let us first examine the case where no noise is present, and how S might be reconstructed using these types of test functions. Evaluating equation (6.6) with the value of v_k in equation (11.1) yields:

$$a_k = -\frac{(1-\gamma)k}{\cosh(k)} \int_0^\pi \frac{\partial u_0}{\partial x}(x, 0) S(x) \sin(kx)\, dx \tag{11.2}$$

Notice that the integral on the right in equation (11.2) represents the Fourier sine coefficients of $\frac{\partial u_0}{\partial x}(x, 0)S(x)$ with a factor of $\frac{2}{\pi}$ multiplied up front. These Fourier sine coefficients c_k are related to the a_k as

$$c_k = -\frac{2\cosh(k)}{(1-\gamma)k} a_k.$$

Once we've computed the $a_k = RG(v_k)$, we find the c_k as above and write $S(x)$ as the following series:

$$S(x) = \sum_{k=1}^{\infty} c_k \sin(kx) = -\frac{2}{(1-\gamma)} \sum_{k=1}^{\infty} \frac{\cosh(k) a_k}{k} \sin(kx) \tag{11.3}$$

Now suppose u contains noise. That is, $\tilde{u} = u(x, 1) + \varepsilon(x)$, where $\varepsilon(x)$ is

some error. We then obtain a corrupted version $\tilde{a}_k$ of the a_k, as

$$\begin{aligned}
\tilde{a_k} &= \int_0^\pi \tilde{u}\frac{\partial v_k}{\partial y}(x,1) - v_k(x,1)g\,dx \\
&= \int_0^\pi (u+\varepsilon(x))\frac{\partial v_k}{\partial y}(x,1) - v_k(x,1)g\,dx \\
&= \int_0^\pi u\frac{\partial v_k}{\partial y}(x,1) - v_k(x,1)g\,dx + \int_0^\pi \varepsilon(x)\frac{\partial v_k}{\partial y}(x,1)\,dx \\
&= a_k + \underbrace{\int_0^\pi \varepsilon(x)\frac{\partial v_k}{\partial y}(x,1)\,dx}_{\varepsilon_k} \qquad (11.4)
\end{aligned}$$

where the second term in equation (11.4) will be denoted ε_k.

Let us bound ε_k. We have

$$\begin{aligned}
\varepsilon_k &= \int_{-M}^{M} \varepsilon(x)\frac{\partial v_k}{\partial y}(x,1)\,dx \\
&= k\int_{-M}^{M} \varepsilon(x)\cos(kx)\frac{\sinh(k)}{\cosh(k)}\,dx
\end{aligned}$$

where $[-M, M]$ is the region where S is supported. But $-1 \le \tanh(k) \le 1$ and $-1 \le \cos(kx) \le 1$. So we now have:

$$\varepsilon_k \le 2kM\varepsilon_\infty \qquad (11.5)$$

where ε_∞ is the supremum of $|\varepsilon|$ over $[-M, M]$.

Now our reconstruction $\tilde{S}$ of the back surface from noisy data based on a Fourier sine expansion will be

$$\begin{aligned}
\tilde{S}(x) &= -\frac{2}{(1-\gamma)}\sum_{k=1}^{\infty}\frac{\cosh(k)\tilde{a}_k}{k}\sin(kx) \\
&= S(x) - \frac{2}{(1-\gamma)}\sum_{k=1}^{\infty}\frac{\cosh(k)\varepsilon_k}{k}\sin(kx) \qquad (11.6)
\end{aligned}$$

Equation (11.6) shows clearly that $\tilde{S}$ may bear little resemblance to S: the presence of the rapidly growing sequence $\cosh(k)/k$ in the summand above, in conjunction with the fact that the ε_k are only bounded weakly, by (11.5) (and in particular, probably won't go to zero) causes the sum on the right to "blow up" as the upper limit of summation increases. Thus, the more terms in the series that are considered, the greater effect the error has on the resulting S function, which clearly demonstrates the ill-posedness of this inverse problem.

12 Regularization

Can we still obtain an accurate approximation despite the effects of error? In this case, we will use Singular Value Decomposition to obtain the accurate approximation. If A is an mxn real-valued matrix, then A can be written in the following way using the Singular Value Decomposition:

$$A = UDV^T$$

where U and V are orthogonal matrices, and D only has entries on the diagonal. Recall equation (5.5). Since the $RG(v_k)$ values are calculable, we will again refer to them as a_k. Also, recall the following numerical method for recovering S:

$$S(x) = \sum_{j=1}^{n} c_j w_j(x) \tag{7.3}$$

where c_j is related to a_k in the following way:

$$a_k = \sum_{j=1}^{n} c_j \int_{-\infty}^{\infty} w_k(x) w_j(x)\, dx, \text{ from } k = 1...n$$

Writing this system in matrix form, we have:

$$A\vec{c} = \vec{a} \tag{12.1}$$

where the entries in $\vec{c}$ are the coefficients in the linear approximation of S.

We will now perform a Singular Value Decomposition on the matrix A. That is:

$$A = UDV^T \tag{12.2}$$

where U and V are orthogonal matrices, ie. $UU^T = I$ and $VV^T = I$ where I is the identity matrix, and D is a diagonal matrix, probably with some singular values close to 0. Substituting the decomposed version of A into equation (12.1) we have:

$$\begin{aligned} UDV^T\vec{c} &= \vec{a} \\ DV^T\vec{c} &= U^T\vec{a} \\ V^T\vec{c} &= D^{-1}U^T\vec{a} \\ \vec{c} &= VD^{-1}U^T\vec{a} \end{aligned} \tag{12.3}$$

Now, assume there is error in u (but, for simplicity only, no error in g). This error is quantified as

$$\tilde{u} = u + \varepsilon$$

where ε is some error function on the top surface. Then the equation for computing the a_k from the boundary data,

$$a_k = \int_\Gamma \left(u \frac{\partial v_k}{\partial \vec{n}} - v_k g \right) ds$$

becomes

$$\tilde{a}_k = a_k + \varepsilon_k \quad = \quad \int_\Gamma \left((u + \varepsilon) \frac{\partial v_k}{\partial \vec{n}} - v_k g \right) ds \tag{12.4}$$

Now subtracting a_k from both sides and taking absolute values, we have:

$$\begin{aligned} |\varepsilon_k| &= \left| \int_{-\infty}^{\infty} \varepsilon(x) \frac{\partial v_k}{\partial \vec{n}}(x, 0)\, dx \right| \\ &\leq \varepsilon_\infty \int_{-\infty}^{\infty} \left| \frac{\partial v_k}{\partial \vec{n}}(x, 0) \right| dx \\ &\leq C \varepsilon_\infty \end{aligned} \tag{12.5}$$

where C is the value of $\int_{-\infty}^{\infty} \left| \frac{\partial v_k}{\partial \vec{n}}(x, 0) \right| dx$ and ε_∞ is the supremum of the error function ϵ_k. This puts a bound on the error ε_k. Writing a system analogous to that in equation (12.1), we have:

$$A(\vec{c} + \vec{c_\varepsilon}) = \vec{a} + \vec{\varepsilon} \tag{12.6}$$

where $\vec{c_\varepsilon}$ is the error in the c_j and ε is all the ε_k errors. We will now subtract equation (12.1) from equation (12.6) to obtain:

$$A\vec{c_\varepsilon} = \vec{\varepsilon} \tag{12.7}$$

which quantifies the error associated with the system.

We will now perform another Singular Value Decomposition on A, and substitute it into equation (12.7).

$$\begin{aligned} UDV^T \vec{c_\varepsilon} &= \vec{\varepsilon} \\ DV^T \vec{c_\varepsilon} &= U^T \vec{\varepsilon} \\ V^T \vec{c_\varepsilon} &= D^{-1} U^T \vec{\varepsilon} \\ \vec{c_\varepsilon} &= V D^{-1} U^T \vec{\varepsilon} \end{aligned} \tag{12.8}$$

Note that multiplication of one vector by orthogonal matrices does not change the length of the original vector (as measured by the usual Pythagorean norm). Thus, the only operation performed above that affects the magnitude of the error is the multiplication by D^{-1}. Recall that D is a diagonal matrix which may have singular values close to 0. As such, D^{-1} may have very large entries along the diagonal. This greatly magnifies the error present in the calculation. To minimize this magnification, we will select a threshold number. All corresponding singular values in the matrix D that are not within this threshold of the largest value of D will be rounded to 0 in D^{-1}, thus lessening the magnification due to D^{-1}.

Now a new problem arises: how do we select this threshold number to get the least error-filled approximation? Recall equation (12.5):

$$\varepsilon_k \leq C\varepsilon_\infty$$

thus we have a bound on all ε_k. The vector $\vec{\varepsilon}$ has entries ε_k from $k = 1$ to n, where n is the number of test functions used. Each of these ε_k is at most equal to $C\varepsilon_\infty$ in magnitude. Thus we now have:

$$\begin{aligned} \|\vec{\varepsilon}\| &\leq \sqrt{nC^2\varepsilon_\infty^2} \\ &\leq \sqrt{n}C\varepsilon_\infty \end{aligned} \tag{12.9}$$

where ε_∞ and C are defined as above. Thus the maximum size of $\|\vec{\varepsilon}\|$ is $\sqrt{n}C\varepsilon_\infty$, which we denote by ε_{max}. We will plot the w_j, and determine the average maximum height, which we denote by h_w. We must then decide how much relative error $\varepsilon_S \in (0, 1)$ we will tolerate in our estimate of S, in the sense that we want $\varepsilon_S \leq \varepsilon_c h_w$, where ε_c is the error in the $\vec{c_\varepsilon}$ coefficients. It thus makes sense to choose

$$\varepsilon_c \approx \frac{\varepsilon_S}{h_w}$$

Recall from equation (12.8):

$$DV^T\vec{c_\varepsilon} = U^T\vec{\varepsilon}$$

The error in $V^T\vec{c_\varepsilon}$ is ε_c. The error in $U^T\vec{\varepsilon}$ is ε_{max}. Let the threshold in the D matrix be denoted by ε_D. Based on equation (12.8) we want $(\varepsilon_D)(\varepsilon_c) \approx \varepsilon_{max}$ or

$$\varepsilon_D = \frac{\varepsilon_{max}}{\varepsilon_c} \tag{12.10}$$

In summary, the entries in the D matrix must be larger than ε_D. That is, if any singular value λ in D is below the threshold ε_D, simply use 0 in place of $1/\lambda$ in the computation (12.3).

13 The Numerical Example with Regularization

In the section on numerical analysis before regularization (Section 9), we ended up with a solution vector of coefficients c_k, $k = 1, ..., n$ (where n is the number of test functions v_j used) for a linear combination of the w_j functions, giving an extremely oscillatory approximation of the corrosion profile $S(x)$ (see Figure 6). We can now use our method of regularization to minimize the oscillatory nature of our approximation of S by using threshold in (12.10). The example is this section is still based on the linearized version of the problem, equations (6.8)-(6.10) and equation (6.7).

In the tests from Section 9, we can calculate the condition number of the matrix B (as defined in (8.2)), which is the ratio of its largest singular value, S_{max}, to its smallest. The larger the condition number, the more ill-conditioned the matrix, yielding more extreme coefficients in the solution $\vec{c}$ (and thus more extreme oscillations in the function produced to approximate S). Before regularization, the condition number of the matrix B could be as high as on the order of 10^{22} with only 11 test functions, with the resultant function $S(x)$ yielding values up to the order of 10^{20}, much too large to produce any useful approximation of the corrosion profile (recall that, for our theoretical purposes, the range of y is $[0, 1]$).

In contrast, a graph of the function created using our regularization technique, with the same measured data and test functions as in Section 9, using calculated threshold $t = 0.26$, can be seen in Figure 7. The oscillations here are less extreme, and the range of values much smaller (on the order of 10^{-1}), giving a much more reasonable image of the corrosion profile $S(x)$.

14 Further Examples

In this section, we present the results from two other tests. The first test was conducted using data generated without any noise, but based on the linearized forward problem (6.8)-(6.10) and equation (6.7); the second was conducted with

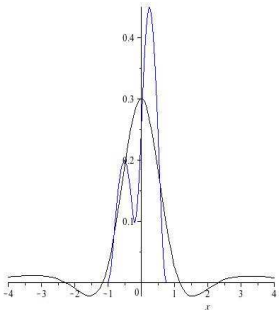

Figure 7: A graph of the approximated corrosion profile with parameters and generated data from Section 9. The black curve is the approximated curve S; the blue curve is the actual corrosion profile used to generate the data.

data generated by solving the fully non-linear forward problem in Section 2, with Comsol's Multiphysics package.

14.1 A Numerical Example without Noise

We show here an example conducted using 200 data points generated with the linearized problem, but with no noise added. We used an input flux g given by

$$g(x) = \frac{\partial u_0}{\partial \vec{n}}(x, 1),$$

where u_0, the function of electrical potential in the case with no corrosion, was given by:

$$u_0(x, y) = \text{Im}\left(\frac{1}{(x + iy - 2i)^2} + \frac{1}{(x - iy - 2i)^2}\right)$$

The function u_0 is harmonic, with normal derivative equal to 0 along the back surface $y = 0$, and real-valued. For a graph of $u(\Gamma) - u_0(\Gamma)$, using this u_0 function and the measured data points u along Γ, see Figure 8.

We assumed the conductivity in the corroded region to be $\gamma = 0.1$. The test functions v_j each had the general form

$$v_j(x, y) = \text{Im}\left(\frac{1}{\frac{10j+n-11}{n-1} - 6 + x + iy - 2i} + \frac{1}{\frac{10j+n-11}{n-1} - 6 + x - iy - 2i}\right).$$

A graph of the approximated corrosion profile (without regularization) with these parameters and with 21 test functions v_j is plotted against the actual

corrosion profile in Figure 9. In this case, the unregularized approximation was sufficient, due to the lack of noise.

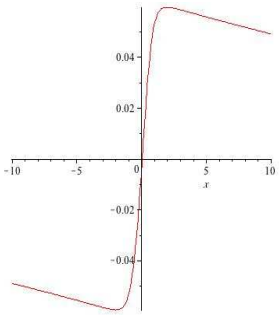

Figure 8: A graph of $u(\Gamma) - u_0(\Gamma)$, using the u_0 and generated data points u from 14.1.

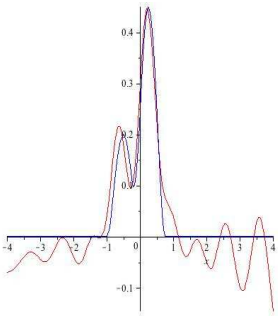

Figure 9: A graph of the approximated corrosion profile with parameters and generated data from Section 14.1 (without regularization). The red curve is the approximated curve S; the blue curve is the actual corrosion profile used to generate the data.

14.2 A Numerical Example with Nonlinear Data

We show here another example conducted using 200 data points generated by Comsol's Multiphysics program to solve the fully nonlinear problem. We used input flux g given by

$$g(x) = \frac{\partial u_0}{\partial \vec{n}}(x, 1),$$

where u_0, the function of electrical potential in the case with no corrosion, was given by:

$$u_0(x, y) = \text{Im}\left(\frac{1}{(x + iy - 2i)^2} + \frac{1}{(x - iy - 2i)^2}\right).$$

As before, the function u_0 is harmonic, with normal derivative equal to 0 along the back surface (where $y = 0$), and real-valued. For a graph of $u(\Gamma) - u_0(\Gamma)$, using this u_0 function and the generated data points u along Γ, see Figure 10.

We again assumed the conductivity in the corroded region to be $\gamma = 0.1$. The test functions v_j each had the general form

$$v_j(x, y) = \text{Im}\left(\frac{1}{\frac{10j+n-11}{n-1} - 6 + x + iy - 2i} + \frac{1}{\frac{10j+n-11}{n-1} - 6 + x - iy - 2i}\right).$$

A graph of the approximated corrosion profile (before regularization) with these parameters is plotted against the actual corrosion profile in Figure 11.

Notice again the extreme oscillations in the approximation before we employed our method of regularization.

A graph of the approximated corrosion profile after regularization, with the same parameters as in Figure 11 and with calculated threshold value $t = 0.42$, is plotted against the actual corrosion profile in Figure 12.

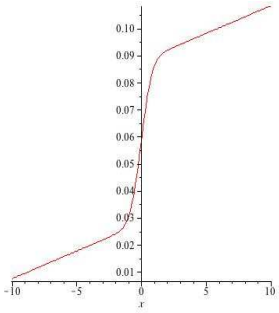

Figure 10: A graph of $u(\Gamma) - u_0(\Gamma)$ with data generated from Comsol Multiphysics solving the fully nonlinear problem.

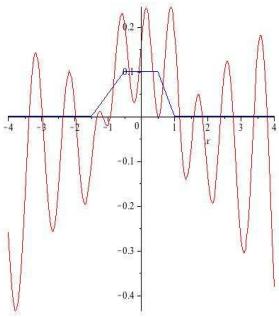

Figure 11: A graph of the approximated corrosion profile using data generated by solving the nonlinear problem (before regularization). The red curve is the approximated curve S; the blue curve is the actual corrosion profile used to generate the data.

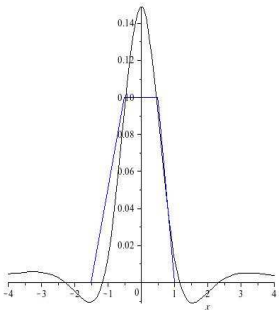

Figure 12: A graph of the approximated corrosion profile using the same data as in Figure 11, after regularization. The black curve is the approximated curve S; the blue curve is the actual corrosion profile used to generate the data.

15 Conclusion and Future Work

Consider a two-dimensional region, Ω, with an accessible surface, Γ, and an inaccessible back surface that is partially corroded. We have shown that it is possible to reconstruct the profile of this corrosion using measurements of electrical potential on Γ. The methods for this reconstruction prove to be fairly accurate considering the ill-posedness of the inverse problem. Ill-posedness was investigated through error analysis, and mitigated with a regularization procedure. We have also shown that, although a unique solution cannot be presented with only one reading of electrical potential on Γ, if two corrosion profiles generate the same potential data along Γ they must have a non-zero point of intersection on their supported domains.

We would like to investigate other aspects of this problem in the future. First, we would like to test the precision of our algorithm. The numerical tests we performed were all done with one section of corrosion on the back surface of Ω. We would like to see how our algorithm handles the presence of two corrosion profiles. How close together can the profiles be before the algorithm no longer recognizes them as two separate entities?

We would also like to improve our algorithm for the approximation of the function $S(x)$. Although the algorithm we have created approximates the corrosion profile closely, it does not do so exactly. Further precision in determining

the threshold values used in the singular value decomposition regularization procedure may improve the algorithm. Considering the possibility of using a different regularization method may also prove useful in this endeavor.

Extending this problem to electrothermal imaging is also something we want to pursue. Does the generation of heat due to current flow in the corroded region allow the corrosion profile to be reconstructed more easily or accurately? We would like to investigate whether or not solution uniqueness in the fully non-linear case can be proven electrothermally despite the inability to do so with purely electrical data.

Ultimately, we would like to extend all of these results to the three-dimensional case where Ω is now a three-dimensional box or rod, and the corrosion profile is a surface. This extension would allow our methods to be used in corrosion detection in the field.

References

[1] Cakoni, F. and Kress, R. "Integral equations for inverse problems in corrosion detection from partial Cauchy data." *Inverse Prob. Imaging* **1** pp. 229-45. 2007.

[2] Strauss, Walter A. *Partial Differential Equations: An Introduction.* pp. 173-174. New York: John Wiley and Sons, Inc. 1992.